The Astrophysical Journal, 627:454–463, 2005 July 1
© 2005. The American Astronomical Society. All rights reserved. Printed in U.S.A.

LIMIT-CYCLE BEHAVIOR IN ONE-ZONE CONVECTIVE MODELS

A. Munteanu,[1] G. Bono,[2] J. José,[3,4] E. García-Berro,[1,3] and R. F. Stellingwerf[5]

Received 2004 April 29; accepted 2005 March 20

ABSTRACT

We present the results of a detailed set of one-zone models that account for the coupling between pulsation and convection following the original prescriptions of Stellingwerf. Motivated by the arbitrary nature of the input parameters adopted in this theoretical framework, we computed several sequences of models that cover a substantial fraction of the parameter space and a longer integration time. We found that our models show the same behavior as nonlinear, hydrodynamic models, that is, they approach either the limit-cycle stability (pulsational instability), the fixed point (pulsational stability), or their present vibrational instability. In agreement with Stellingwerf, we find that convection is the main quenching mechanism for pulsational models located across the Cepheid instability strip. Moreover, our one-zone models can mimic the pulsational behavior of both fundamental and first overtone Cepheids. We also included a turbulent pressure term and found that this physical mechanism plays a crucial role in the pulsation characteristics of the models by removing the sharp discontinuities along the light and the velocity curves shown by models that do not account for turbulent pressure. Finally, we investigated the vibrational and pulsational stability of completely convective models. We consider the most important finding of the present work to be the identification of a well-defined region in the parameter space where they approach limit-cycle stability. The inclusion of turbulent pressure widens this region, thus supporting original suggestions based on both linear and nonlinear models of long period variables (LPVs). Several numerical experiments performed by adopting different values of the adiabatic exponent and of the shell thickness indicate that the coupling between pulsation and convection is the key driving mechanism for LPVs, a finding supported by recent theoretical predictions.

Subject headings: Cepheids — convection — stars: oscillations — stars: variables: other

1. INTRODUCTION

Variable stars are crucial astrophysical objects, since they can be used as tracers of stellar populations in the framework of galaxy evolution (Dolphin et al. 2002; Monelli et al. 2003). Moreover, the comparison between the observables predicted by pulsational models and the observations themselves supplies an independent estimate of the stellar parameters (Bono et al. 2001; Kervella et al. 2001). This implies that stellar pulsations provide a way to probe regions of the star that would be otherwise inaccessible to direct observations. Therefore, variable stars provide the unique opportunity to investigate the plausibility of the physical assumptions adopted to construct both evolutionary and pulsational models (Bono et al. 2002; Keller & Wood 2002).

Nonadiabatic stellar pulsations are complicated phenomena, even for small amplitudes and purely radial oscillations, to which the linear theory is applicable. For large amplitudes, the nonlinear effects become important and the simplifying assumptions must be treated with caution. During the last decades the work on nonlinear stellar pulsations has been developed along three main approaches: simple one-zone models, the formalism of amplitude equations, and hydrodynamic models. Although the third approach provides the most detailed and accurate physical description of the outermost stellar layers during the pulsation cycle, it is also true that it is difficult to figure out whether the intrinsic features of the models are either a direct consequence of the adopted physical assumptions or caused by the numerical methods and the spatial resolution adopted to discretize the stellar structure into a series of concentric shells (see, e.g., Petroni et al. 2003 and references therein). It is within this framework that simple one-zone models (Baker 1966; Saitou et al. 1989; Unno & Xiong 1993; Icke et al. 1992; Tanaka 2001) and the amplitude equation formalism (Dziembowski & Kovacs 1984; Buchler & Kovacs 1986; Ishida & Takeuti 1991; Saitou 1993) play a key role. The advantages and drawbacks of these approaches have already been widely discussed in the literature (see, e.g., Buchler 1998 and references therein; Tanaka 2001). In particular, one-zone models have been introduced with the sole purpose of clarifying the analysis by eliminating possible subtle uncertainties introduced by the stability of numerical algorithms and by spatial resolution. This was accomplished by considering the stellar envelope as a one-zone structure: a single, relatively thin, spherical mass-shell concentric with the stellar center. These models have provided clear understanding of the destabilization mechanisms and of the possible consequences of couplings as well as feedbacks between several phenomena associated with stellar variability (see Baker 1966; Usher & Whitney 1968; Saitou et al. 1989; Unno & Xiong 1993; Icke et al. 1992; Tanaka 2001).

The simplest one-zone model that accounts for the coupling between pulsation and convection was suggested by Stellingwerf (1986). Following the convective scheme developed by Stellingwerf (1982), he derived a one-zone pulsational model that includes a time-dependent convective term. He computed a

[1] Departament de Física Aplicada, Universitat Politècnica de Catalunya, Avenida del Canal Olímpic, s/n, 08860 Castelldefels (Barcelona), Spain; andreea@fa.upc.es, garcia@fa.upc.es.

[2] Osservatorio Astronomico di Roma, Via Frascati 33, 00040 Monte Porzio Catone, Italy; bono@mporzio.astro.it.

[3] Institut d'Estudis Espacials de Catalunya, Edifici Nexus-201, c/ Gran Capità 2-4, 08034 Barcelona, Spain.

[4] Departament de Física i Enginyeria Nuclear, Universitat Politècnica de Catalunya, Avenida Víctor Balaguer, s/n, 08800 Vilanova i la Geltrú (Barcelona), Spain; jordi.jose@upc.es.

[5] Stellingwerf Consulting, 2229 Loma Linda, Los Alamos, NM 87544; rfs@stellingwerf.com.

set of models associated with the Cepheid instability strip, integrating them only for a few dynamical timescales. The results of this work support the generally accepted view that convection is a damping mechanism, particularly for models located close to the cool edge of the instability strip. Although the pulsationally unstable region and the velocity curves were in qualitative agreement with empirical data, he also found that fully convective models underwent vibrational instability for certain values of the parameters. A similar approach was also adopted by Unno & Xiong (1990, 1993) and by Saitou (1993), but they did not discuss in detail the pulsational and dynamical behavior of their models.

In this work, we present new results and possible extensions of the one-zone model developed by Stellingwerf (1986), investigating the limit-cycle behavior (pulsational instability) and accounting for the role of the turbulent pressure and of the thickness of the convective layer. The paper is organized as follows. In § 2 we present the one-zone convective model. We place special emphasis on the adopted physical and numerical assumptions. In § 3 we thoroughly investigate the limit-cycle behavior of the model suggested by Stellingwerf (1986), an issue marginally addressed in the original paper. In this section we also focus our attention on the dependence of pulsation properties on the shell thickness (§ 3.1) as well as on the turbulent pressure (§ 3.2) and their role in determining the morphology of light and velocity curves. In § 4 we discuss the approach to limit-cycle stability of completely convective models and briefly describe possible empirical similarities with LPVs. Finally, in § 5 we summarize our main results and briefly outline future perspectives. In the Appendix we discuss in more detail the physical assumptions adopted to include the turbulent pressure in the one-zone model.

2. THE ONE-ZONE CONVECTIVE MODEL

In the classical theoretical framework of one-zone models, variable stars have an equilibrium radius R_0 and an extended shell or envelope of variable radius R on top of a compact core of radius R_c. As detailed in Stellingwerf (1986), by accounting for the equation of motion, the energy equation, and the equation of convective transport, the resulting dynamical system describes the evolution of the convective upper layer, and it has the following form:

$$\frac{d^2X}{d\tau^2} = HX^{-q} - X^{-2},$$
$$\frac{dH}{d\tau} = \zeta X^{2d}\left(1 - \gamma_r X^b H^{s+4} - \gamma_c X^{-c} U_c^3\right),$$
$$\frac{dU_c}{d\tau} = \zeta_c\left(X^{-d}H^{1/2} - U_c\right), \qquad (1)$$

where X and H are the radius and the nonadiabatic pressure normalized to their equilibrium values, respectively, while U_c is related to the convective velocity and is defined as $U_c \equiv U'/U_{\mathrm{ml}_0}$, where U_{ml_0} is the equilibrium mixing-length convective velocity. Moreover, the time variable τ is normalized to the dynamical (free fall) timescale. As defined in Stellingwerf (1986), the other input parameters of the model are $q \equiv m\Gamma_1 - 2$, $d \equiv m(\Gamma_1 - 2)/2$, and $c \equiv m - 2$, where Γ_1 is the adiabatic exponent and m is the so-called form factor. In the limit of small oscillations (Stellingwerf 1972, 1986), the form factor is defined as

$$m = \lim_{X\to 1} \frac{\log[(X^3 - \eta^3)/(1 - \eta^3)]}{\log(X)} = \frac{3}{1 - \eta^3}, \qquad (2)$$

with $\eta \equiv R_c/R_0$. At the same time, $b \equiv 4 + m[n - (s + 4)(\Gamma_1 - 1)]$, where s and n are the temperature and the density exponents in the Kramers opacity law, respectively (for more details, see Baker 1966).

The main control parameters of the model are ζ, ζ_c, and γ_c, which are defined as follows: (1) the nonadiabatic parameter, ζ, is the ratio between the dynamical and the thermal timescale; (2) the convective efficiency, ζ_c, is the ratio between the dynamical time and the convective timescale; and (3) the convective-radiative splitting, γ_c, is the ratio between the initial convective luminosity and the total initial luminosity, that is, $\gamma_c \equiv L_{c_0}/L_0$, which implies that $\gamma_r = 1 - \gamma_c$.

The reader interested in a detailed discussion concerning the convective timescale in the context of one-zone models is referred to § 4 of Stellingwerf (1986). More quantitative predictions concerning the different timescales connected with turbulent energy across the envelope of variable stars have been provided by Stellingwerf (1982), Bono et al. (1999), and Feuchtinger et al. (2000).

The values $n = 1$ and $s = 3$ for the Kramers opacity are the standard ones, while the values for Γ_1, m, γ_c, ζ, and ζ_c must be treated with caution. The value of $\Gamma_1 = 1.1$ adopted in Stellingwerf (1986) is a typical value for the γ-mechanism operating in the partial ionization regions (Cox 1980). The choice of a form factor m equal to 10 ($\eta = 0.888$), considered typical of Cepheids in Stellingwerf (1986), together with the values chosen for the other parameters assure the turbulent stability and the secular stability for ζ and ζ_c in the range [0, 10] and $\gamma_c \leq 1$ (Stellingwerf 1986). The values of these parameters were arbitrarily chosen by Stellingwerf (1986) and lead to the existence of a pulsationally unstable region ("strip") for values of $\gamma_c \leq 0.45$. From a mathematical point of view, we refer to such a behavior as having a limit cycle born through a Hopf bifurcation. The stability analysis in Stellingwerf (1986) was hampered by the fact that individual models were integrated only for a small number of dynamical timescales. In particular, our calculations show that for these cases, no limit-cycle stability exists. Note also that Stellingwerf (1986) analyzed only the cases for ζ and $\zeta_c \leq 4$ and that an exhaustive study of the dependence of the limit-cycle behavior on the input parameters remained to be performed.

In the current investigation, we have first undertaken a thorough study of the dynamics in the (ζ, ζ_c)-plane for ζ and $\zeta_c \leq 10$ and for different values of the convective-radiative splitting, γ_c, following the assumption of radiative-dominated energy transport ($\gamma_c \leq 0.5$). We have used the same form factor ($m = 10$) and the same initial condition $(X_0,\ V_0,\ H_0,\ U_{c_0}) = (1.4,\ 0.0,\ 1.0,\ 0.7)$ adopted by Stellingwerf (1986). We have furthermore assumed that a case is pulsationally unstable (limit-cycle behavior) when two consecutive maxima in radius variations differ by less than 10^{-7} and pulsationally stable (damping oscillations) when the solution asymptotically approaches the fixed point $(\bar{X},\ \bar{V},\ \bar{H},\ \bar{U}_c) = (1,\ 0,\ 1,\ 1)$ and its distance to the fixed point becomes smaller than 10^{-8}. The solution was considered to be vibrationally unstable when the rapidly increasing dimensionless radius amplitude became larger than 15. These thresholds are reasonable values. Moreover, we have also verified that the resulting qualitative dynamics does not depend on the choice of these values. Of course, one could use as well the asymptotic perturbation theory to compute the properties of the limit cycle. Nevertheless, such an approach is beyond the aims of the current investigation, and we consider it as a future line of work. For a better understanding of our results, we illustrate in Figure 1 the three types of dynamical behavior we have identified.

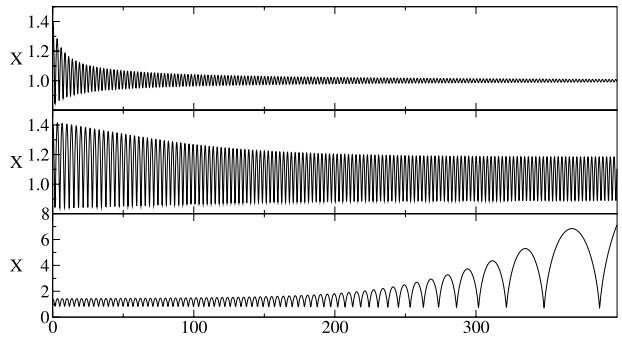

FIG. 1.—Examples of dynamical behavior for $\gamma_c = 0.4$. Radius time series for stable [$(\zeta_c,\ \zeta) = (3,\ 4)$; *top*], limit-cycle [$(\zeta_c,\ \zeta) = (1.5,\ 1.5)$; *middle*], and unstable behavior [$(\zeta_c,\ \zeta) = (0.5,\ 0.5)$; *bottom*].

The top panel shows an example of pulsational stability, i.e., the initial perturbation decays. The bottom panel shows a vibrationally unstable model (the initial perturbation grows), while the middle panel shows the time series of a case that approaches a limit-cycle stability (pulsational instability). Note that for small amplitudes ($\tau \leq 100$) the case plotted in the bottom panel seems to approach a limit cycle, but for $\tau > 200$ it becomes clear that the amplitudes are steadily increasing. This finding further strengthens the need for long time integrations to assess the type of stability for the individual one-zone models. As a final comment on the numerical assumptions considered in the present work, it is worth mentioning that the dynamical behavior of the system is independent of the initial condition, provided that it belongs to the neighborhood of the fixed point $(\bar{X},\ \bar{V},\ \bar{H},\ \bar{U}_c) = (1,\ 0,\ 1,\ 1)$. Therefore, we did not investigate the dependence of the characteristics of the time series on initial conditions.

3. LIMIT-CYCLE CHARACTERISTICS

One-zone models can be adopted to perform only a qualitative comparison with pulsation properties of variable stars. Moreover, this comparison is limited to observables that one-zone models can account for, in particular, the shape of light and velocity curves—originally suggested for RR Lyrae stars by Stellingwerf & Donohoe (1986)—and the occurrence of first overtone pulsators (Stellingwerf et al. 1987). The most interesting results disclosed by our simulations are presented in Figures 2*a*–2*e*, where the regions of damped oscillations are shown in gray, the regions where the radial displacements approach a limit cycle are marked in black, and vibrationally unstable cases are shown in white. A glance at the data plotted in Figure 2 discloses that with the exception of the case in which $\gamma_c = 0.1$, an increase in γ_c causes a decrease in the region of pulsationally unstable cases and that for $\gamma_c = 0.5$ it vanishes. These findings support the results originally obtained by Stellingwerf (1986) concerning the damping role of convection. In addition to the radius (X) and velocity (V) curves chosen to be illustrated in Stellingwerf (1986), we have added the light (L) curve and in several occasions the temperature (T) variations, estimated according to

$$L \equiv \frac{L_*}{L_0} = \frac{L_{*r} + L_{*c}}{L_0} = \gamma_r X^b H^{s+4} + \gamma_c X^{-c} U_c^3, \qquad (3)$$

$$\frac{T}{T_0} = X^{-2d} H, \qquad (4)$$

where L_* denotes the stellar luminosity, while the subscripts r and c refer to the radiative and convective components, respectively, as they result from Stellingwerf (1986). Figure 3 shows the light curve L and the radius X and velocity V time series for selected cases that approach limit cycle. Note that to improve the visualization of data plotted in Figure 3, we subtracted from the integration time τ the time interval spent by individual models to approach the limit-cycle stability. We have chosen to illustrate cases at fixed γ_c and ζ_c values and with ζ ranging from 0.7 to 6.5, being typical examples of the qualitative dynamics encountered. The time series plotted in Figure 3 show that the cases characterized by parameters located close to the edge of the pulsational stability region (Fig. 2, *gray area*) present small amplitudes and sinusoidal changes (Fig. 3*a*). These features are quite similar to the behavior that nonlinear, convective models show close to the blue edge of the instability strip (see, e.g., Bono et al. 2000). On the other hand, models that are located across the pulsationally unstable region (Figs. 3*b* and 3*c*) show a bump along the rising branch of the luminosity curve. Our calculations reveal that such a feature is due to the sharp increase in the efficiency of the convective motions, close to the phase of minimum radius. This finding is also found in nonlinear hydrodynamic models.

One can notice that for cases located close to the vibrationally unstable region, the bump becomes very narrow (Fig. 3*d*) and pulselike (Fig. 3*e*). This is a behavior that is not observed in actual Cepheids, and it is not supported by nonlinear, convective models. This indicates the limit of the crude physical and numerical approximations adopted to construct our models. However, our analysis suggests that the limit-cycle behavior of these one-zone models in the pulsationally unstable region mimics the behavior of the classical Cepheids instability strip, as argued in the original paper of Stellingwerf (1986). Finally, we note that the period of the oscillations of the cases plotted in Figure 3 is not unity, even if the dynamical timescale was normalized to unity. This strong nonlinear effect on the period was already noted by Stellingwerf (1986), who suggested that it was due to a

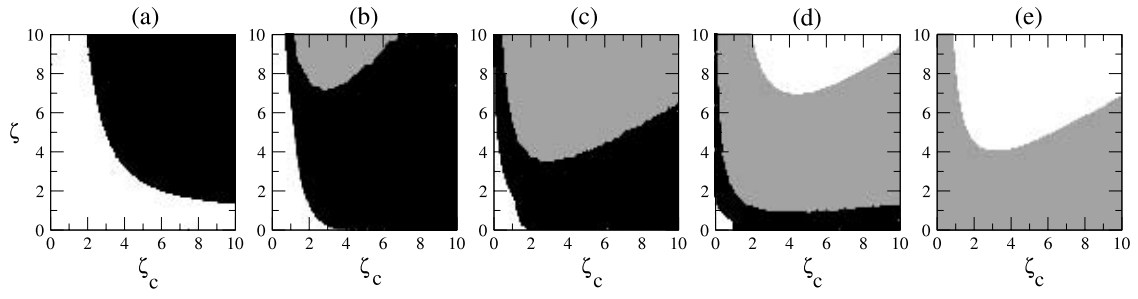

FIG. 2.—The (ζ, ζ_c)-plane for several values of γ_c: (*a*), $\gamma_c = 0.1$, (*b*) $\gamma_c = 0.2$, (*c*) $\gamma_c = 0.3$, (*d*) $\gamma_c = 0.4$, and (*e*) $\gamma_c = 0.5$, representing pulsationally unstable (*black*), pulsationally stable (*gray*), and vibrationally unstable behavior (*white*).

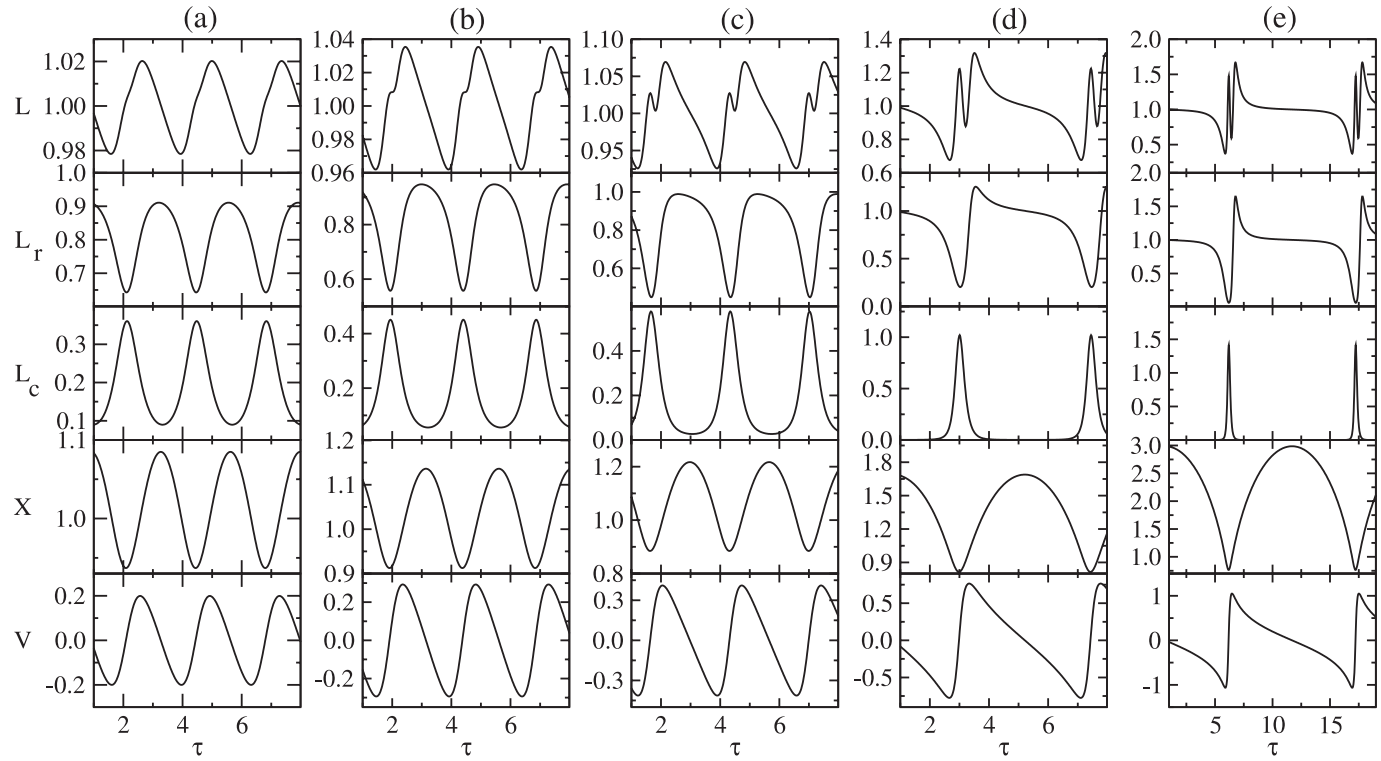

FIG. 3.—Limit-cycle characteristics. From top to bottom the panels show the total luminosity L, the radiative luminosity $L_r \equiv L_{*r}/L_0$, the convective luminosity $L_c \equiv L_{*c}/L_0$, and the dimensionless radius X and velocity V variations. The temporal axis is represented as $\tau - \tau_{lc}$, where τ_{lc} is the time value when the limit cycle has been achieved. The parameters adopted to construct the individual cases were chosen from Fig. 2*b*: (*a*) small amplitude, $(\zeta,\ \zeta_c) = (6.5,\ 3)$; (*b*) bump Cepheid, $(\zeta,\ \zeta_c) = (5.5,\ 3)$; (*c*) double-peak Cepheid, $(\zeta,\ \zeta_c) = (4,\ 3)$; (*d*) steep bump, $(\zeta,\ \zeta_c) = (1.5,\ 3)$; and (*e*) pulselike, $(\zeta,\ \zeta_c) = (0.7,\ 3)$.

correlation with the pulsation amplitude (see also Stellingwerf & Donohoe 1986).

3.1. *The Shell Thickness*

In this section, we present the results concerning the impact of the shell thickness on the existence of limit-cycle behavior and on its characteristics. According to classical physical arguments, pulsational models only account for the envelope of variable stars (Cox 1980). They include a damping, adiabatic region that is typically located on top of the nuclear-burning region (core), a transition region, a driving, nonadiabatic region, and the outermost layers (surface). The driving region is the envelope zone where key elements (hydrogen, helium, and metals) are partially ionized and supply, via the κ- and/or the γ-mechanism, the pulsation destabilization. In this theoretical framework, the base of the envelope in nonlinear, hydrodynamic models is typically located at a few percent of the total radius (Petroni et al. 2003).

As far as the one-zone model approach is concerned, different assumptions have been adopted in the literature. The one-zone model suggested by Icke et al. (1992) for Mira variables accounts for a driving region (piston approximation) at $X \approx 0.2$–0.4, a transition region through which the pressure waves from the interior propagate, and a dissipation region that they call mantle. On the other hand, the one-zone model of Stellingwerf (1986) for variable stars in the Cepheid instability strip accounts for a driving convective region located at $X \approx 0.85$ on top of a damping, adiabatic region ("rigid core"). In this theoretical framework, the pulsation destabilization is provided by a driving agent ($\Gamma_1 < 4/3$). The two different assumptions describe the same envelope region if the rigid core assumed by Stellingwerf (1986) is the outer boundary of the damping region. Therefore, the "shell thickness," $(1 - \eta)$ in dimensionless formulation, is the radial extent of the region located above the boundary between the damping (adiabatic) and the driving (nonadiabatic) region.

To investigate the dependence of the dynamic behavior of the system given in equation (1) on the shell thickness, we have chosen two values of the shell thickness, one smaller and the other larger than the value adopted in Stellingwerf (1986): $\eta = 0.75$ and 0.92. We illustrate in Figures 4 and 5 the behaviors in

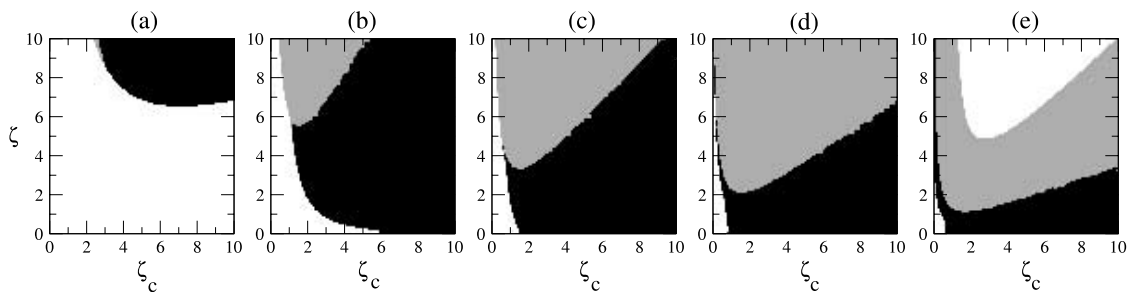

FIG. 4.—The (ζ, ζ_c)-plane for several values of γ_c. Eq. (1) has been used with $\eta = 0.75$: (*a*) $\gamma_c = 0.1$, (*b*) $\gamma_c = 0.2$, (*c*) $\gamma_c = 0.3$, (*d*) $\gamma_c = 0.4$, and (*e*) $\gamma_c = 0.5$, representing pulsationally unstable (*black*), pulsationally stable (*gray*), and vibrationally unstable behavior (*white*).

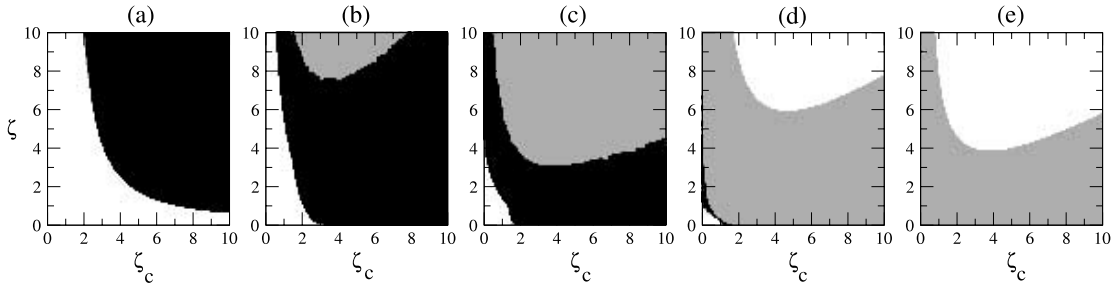

FIG. 5.—The (ζ, ζ_c)-plane for several values of γ_c. Eq. (1) has been used with $\eta = 0.92$: (*a*) $\gamma_c = 0.1$, (*b*) $\gamma_c = 0.2$, (*c*) $\gamma_c = 0.3$, (*d*) $\gamma_c = 0.4$, and (*e*) $\gamma_c = 0.5$, representing pulsationally unstable (*black*), pulsationally stable (*gray*), and vibrationally unstable behavior (*white*).

the (ζ, ζ_c)-plane for $\gamma_c \leq 0.5$. One can notice that the increase in the shell thickness (decrease of η) leads to the existence of pulsational instability for cases characterized by stronger convection (higher values of γ_c). This effect is expected, because a decrease in η implies an increase in the extent of the driving region. Moreover, we have noted that for a fixed value of γ_c and different values of η, the period distribution of the cases that approach a stable limit cycle peaks at shorter periods as the shell thickness decreases. This behavior is also expected, since detailed nonlinear, hydrodynamic models of RR Lyrae (Bono & Stellingwerf 1994) and classical Cepheids (Bono et al. 1999) suggest that the regions located below the nodal line supply a small contribution to the work integral of first-overtone pulsators. This supports the suggestion by Stellingwerf et al. (1987) to decrease the shell thickness of one-zone models in order to mimic the dynamical behavior of overtone pulsators.

3.2. *The Turbulent Pressure*

Convection affects pulsation through three factors, namely, convective energy transfer (thermodynamic coupling), turbulent pressure, and turbulent viscosity (dynamic coupling). The effect of turbulent viscosity is to convert the kinetic energy of radial motions into thermal energy by means of a turbulent cascade of smaller and smaller turbulent eddies. This means that the turbulent viscosity is a pure damping factor (Stellingwerf 1982; Xiong et al. 1998; Yecko et al. 1998). The role that turbulent pressure plays in driving or damping the pulsation is not straightforward, since the contributions of gas and turbulent pressure cannot be easily separated. Linear (Yecko et al. 1998) and nonlinear (Bono et al. 1999) convective models of classical Cepheids suggest that the work done by turbulent pressure attains both positive (driving) and negative (damping) values in different regions of the envelope. Linear and nonlinear convective LPV models constructed by Ostlie & Cox (1986) and by Cox & Ostlie (1993) indicate that turbulent pressure is a driving mechanism, whereas more recent calculations by Xiong et al. (1998) support the evidence that it is a damping mechanism.

The turbulent pressure, P_t, was not included in the original one-zone model by Stellingwerf (1986), but it was briefly mentioned as being

$$\frac{P_t}{P_{t_0}} = X^{-m} U_c^2, \tag{5}$$

where the zero subscript denotes its equilibrium value. In this section, we present the results obtained by the introduction of the turbulent pressure. The reader interested in a detailed description of the physical assumptions adopted to include the turbulent pressure term in equation (1) is referred to the Appendix. The new dynamic system now becomes

$$\begin{aligned}
\frac{d^2X}{d\tau^2} &= (1-\alpha_p)X^{-q}h + \alpha_p X^{-c}U_c^2 - X^{-2}, \\
\frac{dH}{d\tau} &= -m\frac{\alpha_p(\Gamma_3-1)}{1-\alpha_p}X^{2d-1}\frac{dX}{d\tau}U_c^2 \\
&\quad - \zeta X^{2d}\left[\gamma_r X^b h^{s+4} + (1-\gamma_r)X^{-c}U_c^3 - 1\right], \\
\frac{dU_c}{d\tau} &= \zeta_c\left(X^{-d}H^{1/2} - U_c\right).
\end{aligned} \tag{6}$$

We have undertaken a parametric study in order to investigate the influence of the turbulent pressure on the overall dynamics of the system and implicitly on the existence of limit cycles. For this purpose, we have chosen the same initial condition as in § 2, that is, $(X_0,\ V_0,\ H_0,\ U_{c_0}) = (1.4,\ 0.0,\ 1.0,\ 0.7)$, which led to a value of $\alpha_p \approx 0.4$. The results concerning the (ζ, ζ_c)-plane are shown in Figure 6, using the color code from Figure 2. The regions characterized by the existence of limit cycles for $\gamma_c < 0.5$ are more extended than in the case without turbulent pressure, as expected because the additional pressure adds to the driving mechanism.

We have also investigated the light and velocity curves for the cases characterized by limit-cycle behavior. From the hydrodynamic models as well as from plain physical arguments on

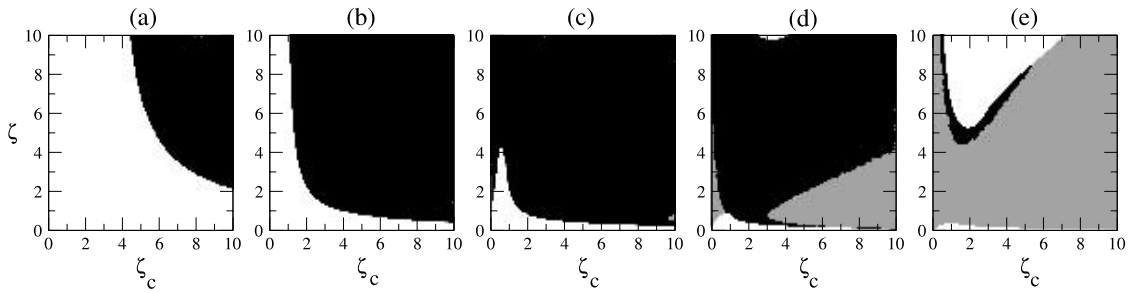

FIG. 6.—The (ζ, ζ_c)-plane for $\eta = 0.888$ and several values of γ_c when the turbulent pressure is included: (*a*) $\gamma_c = 0.1$, (*b*) $\gamma_c = 0.2$, (*c*) $\gamma_c = 0.3$, (*d*) $\gamma_c = 0.4$, and (*e*) $\gamma_c = 0.5$, representing limit-cycle (*black*), stable (*gray*), and vibrationally unstable behavior (*white*).

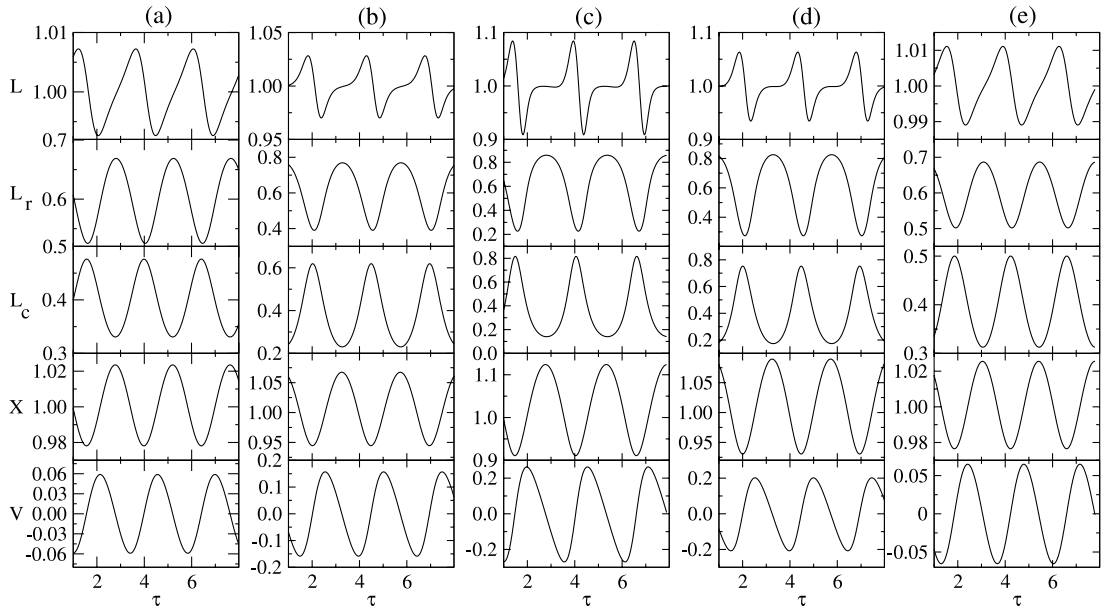

FIG. 7.—Limit-cycle characteristics when the turbulent pressure is introduced. From top to bottom the panels show the total luminosity L, the radiative luminosity $L_r \equiv L_{*r}/L_0$, the convective luminosity $L_c \equiv L_{*c}/L_0$, and the radius X and the velocity V variations. The temporal axis is represented as $\tau - \tau_{\rm lc}$, where $\tau_{\rm lc}$ is the time value when the limit cycle has been achieved. The parameters adopted to construct the individual cases are $\eta = 0.888$; $\gamma_c = 0.4$; and (*a*) $(\zeta,\ \zeta_c) = (4,\ 0.28)$, (*b*) $(\zeta,\ \zeta_c) = (4,\ 0.4)$, (*c*) $(\zeta,\ \zeta_c) = (4,\ 1)$, (*d*) $(\zeta,\ \zeta_c) = (4,\ 4)$, and (*e*) $(\zeta,\ \zeta_c) = (4,\ 9)$.

the existence of the Cepheid instability strip, it is expected that by crossing the instability strip from the blue to the red edge, the period increases and the amplitude of the oscillations quickly reaches its maximum and then slowly decreases. In order to obtain a similar evolution of the amplitude from this one-zone model, the limit-cycle region must be bounded in the $(\zeta,\ \zeta_c)$-plane by pulsationally stable regions both to the left (low values of ζ_c) and to the right (high values of ζ_c). If bounded by a vibrationally unstable region, the oscillations that result from using parameters close to this boundary are pulselike and the amplitude is large, as in Figure 3*e*. One can notice that for the case of zero turbulence pressure, the limit-cycle region is bounded to the left by the vibrationally unstable behavior, and thus the above condition is not satisfied. However, with the introduction of the turbulent pressure, there exists a case for which the limit-cycle region is bounded in the $(\zeta,\ \zeta_c)$-plane both to the left and to the right by the pulsationally stable behavior (Fig. 6*d*). For this case, we present in Figure 7 the types of light and velocity curves obtained in the transition from the hot (blue, low ζ_c) to the cool (red, high ζ_c) edge, at constant ζ. One can notice that the amplitude has a peak toward the center of the limit-cycle region and then it decreases. Even more importantly, data plotted in Figure 7 disclose that one-zone models that account for turbulent pressure do not present, in this region of the parameter space, the spurious secondary peak along the rising branch. The morphology of light and velocity curves plotted in Figure 7 are in qualitative agreement with actual classical Cepheids and with nonlinear, convective models.

4. THE RED VARIABLES

Stellingwerf (1986) remarked on a paradox of the present one-zone model: "although the convection tends to stabilize the pulsation in the majority of cases, the completely convective case shows instability in every criterion." We have verified that indeed the present model with a fully convective ($\gamma_c = 1$) thick shell ($m < 8$ or $\eta < 0.85$) presents vibrational instability for any $\zeta,\ \zeta_c \leq 10$. However, for a thin shell, our simulations revealed that while no limit-cycle regions exist for the cases with $0.5 \lesssim \gamma_c < 1.0$ and $\zeta,\ \zeta_c \leq 10$, limit-cycle models exist for the case of fully convective shells. Figure 8*a* shows the $(\zeta,\ \zeta_c)$-plane for $\gamma_c = 1.0$, $\eta = 0.888$ and without turbulent pressure. Although the current analysis relies on simple one-zone models, this is a very interesting finding, and we are tempted to attribute this region of the $(\zeta,\ \zeta_c)$-plane to the instability strip of LPVs—variable red giants and supergiants—which are thought to be significantly nonadiabatic and highly convective. There is general agreement within the astrophysical community that the intrinsic reason for the existence of the red edge of the Cepheid instability strip is the damping produced by convection. However, theoretical and empirical evidence suggest that convection might also be a destabilizing mechanism in the cool region of the H-R diagram (Fox & Wood 1982; Edmonds & Gilliland 1996; Xiong et al. 1998; Wood 2000; Christensen-Dalsgaard et al. 2001; Dziembowski et al. 2001; Kiss & Bedding 2003; Ita et al. 2004). When the convective timescale is much longer than the dynamical timescale ($\zeta_c \ll 1$), the effect of convection is stabilizing, but when the convective timescale is much shorter, the reverse is true (Gough 1967). Thus, it may provide an important driving mechanism in red giants and supergiants. More precisely, the convective luminosity in the ionization regions of red pulsating variables is expected to exceed 99% of the total luminosity, as mentioned by Xiong et al. (1998). They identify a Mira instability strip outside the Cepheid instability strip when pulsation-convection interaction is taken into account.

To investigate the effect of the turbulent pressure in the case of a completely convective shell, we have identified in the $(\zeta,\ \zeta_c)$-plane the regions characterized by limit-cycle behavior. We illustrate the results in Figure 8*b*. The region of limit cycles for the completely convective case persists when the turbulent pressure is introduced. Compared to the cases with no turbulent pressure, this region shifts to smaller values of the convective efficiency,

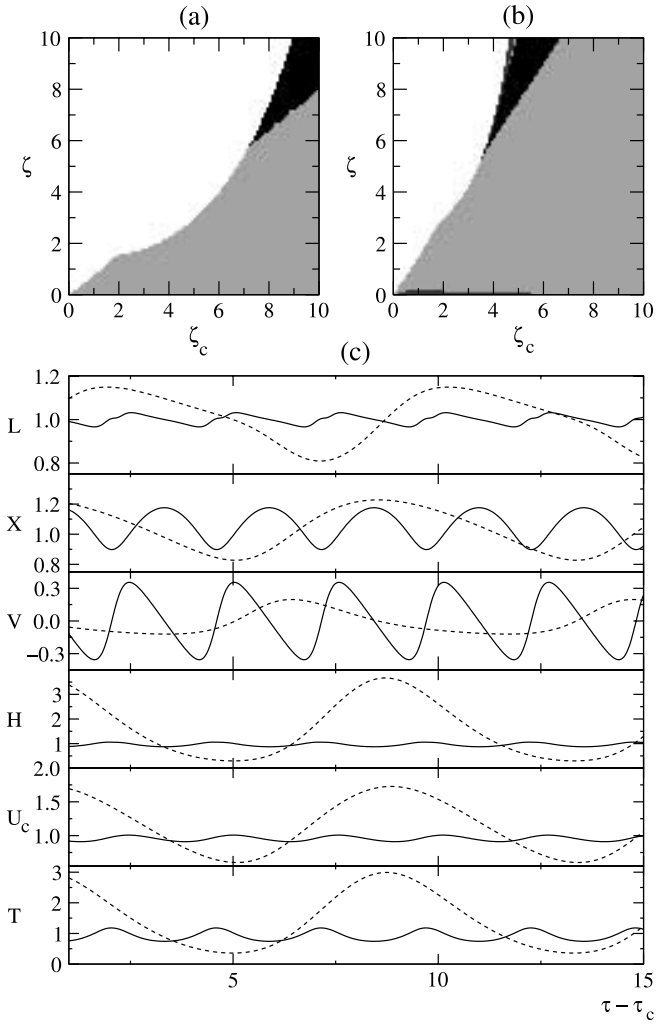

FIG. 8.—The (ζ, ζ_c)-plane for the completely convective shell illustrated in the spirit of Fig. 2 for $\gamma_c = 1.0$ and $\eta = 0.888$ and (*a*) for no turbulent pressure and (*b*) with turbulent pressure included. (*c*) Time series for the luminosity L, radius X, velocity V, pressure H, convective velocity U_c, and temperature T for a Cepheid-like (*solid line*: $\gamma_c = 0.2$, $\zeta_c = 1.2$, $\zeta = 8$) and a LPV-like variable star (*dashed line*: $\gamma_c = 1.0$, $\zeta_c = 9$, $\zeta = 7.5$); the latter case was extracted from (*a*).

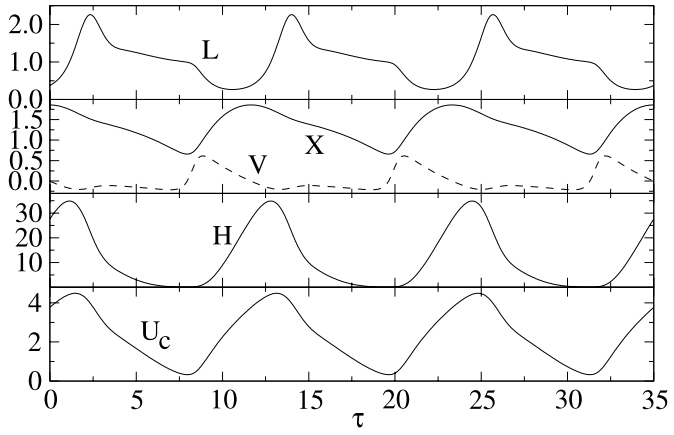

FIG. 9.—Variation of the luminosity L, radius X, velocity V, pressure H, and convective velocity U_c, for the case of completely convective shell close to the vibrationally unstable edge ($\zeta_c = 8.7$, $\zeta = 9$). The case of zero turbulent pressure was considered.

ζ_c. This shift occurs because the minimal perturbation strength necessary to drive the pulsational instability is achieved at weaker convective driving (smaller ζ_c), as the rest of the driving is now provided by the turbulent pressure.

Before verifying that convection is the driving agent for the completely convective shell, we briefly describe the pulsation characteristics of the models constructed by adopting $\gamma_c = 1.0$ and compare them with the previously discussed limit cycles. For comparative purposes, Figure 8*c* shows the time series of a "Cepheid" ($\gamma_c < 0.5$) and of a "LPV" model ($\gamma_c = 1.0$). The increase both in period and amplitude observed in this figure when passing from a Cepheid-like to a LPV-like model supports the previous working hypothesis. In this context it is worth mentioning that Cepheid-like pulsators show the well-known phase lag between the light and the velocity curve. The pulsation behavior of the LPV-like model needs to be discussed in more detail. The data plotted in the top and bottom panels show a very small phase lag between the light and the temperature changes. This evidence appears to be supported by infrared spectroscopic data (Hinkle et al. 1982, 1984) of pulsating asymptotic giant branch (AGB) stars. However, the maximum in the light curve takes place before the minimum in the velocity curve. This finding is at odds with observational data for Mira and semiregular variables, since the minimum velocity is not correlated with light maxima (Hinkle et al. 1982; Lebzelter et al. 2000; Lebzelter & Hinkle 2002). Nevertheless, the comparison between theory and observations is hampered by the occurrence of long secondary periods (Hinkle et al. 2002; Wood et al. 2004), and indeed in a few objects the minimum in the velocity curve takes place later than the maximum in the velocity curve—χ Oph, R Leo (Hinkle et al. 1984), and S Lep (Wood et al. 2004). In passing we would also like to draw attention to the correlation between light maxima and convective velocity, since the maximum takes place just before maximum light. We are not aware of macroturbulent velocity measurements in LPVs, and new observations would be very useful to constrain the plausibility of the physical assumptions adopted in simple one-zone convective models.

For completeness, we illustrate in Figure 9 the time behavior of a model located close to the vibrational instability edge after approaching limit-cycle stability. This example is generic for all the cases with or without the turbulent pressure close to the vibrational-instability edge for the completely convective shell. The data plotted in Figure 9 show a well-defined bump along the decreasing branch of the light curve. This bump becomes more pronounced as the values of the parameters ζ and ζ_c approach the vibrational-instability edge, while the peak of the luminosity becomes a pulselike feature. The occurrence of such secondary features is quite typical along the light curves of Mira variables (Wood et al. 2004). Moreover, the occurrence of the luminosity maximum appears strongly correlated with the variation of the convective velocity U_c, while the bump is in phase with the change of the radial velocity V.

Similar to the limit cycles for the weakly convective cases associated with the classical Cepheids, it is highly speculative to attribute specific values of the parameters ζ and ζ_c to different types of LPVs. A more detailed investigation of the parameter space is mandatory to pinpoint the pulsation properties of completely convective one-zone models that mimic red giant branch–like or Mira-like behavior.

4.1. *The γ-Mechanism*

As a natural further step into clarifying the origin of the pulsationally unstable cases for the completely convective shell, we

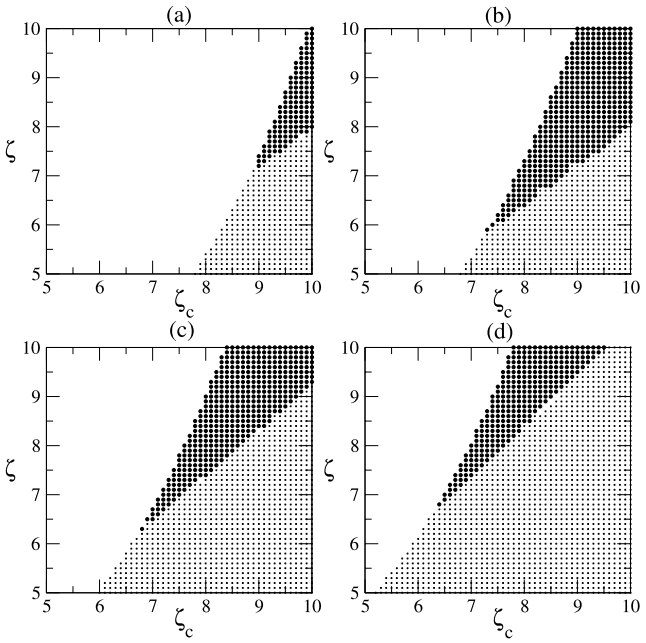

FIG. 10.—The (ζ, ζ_c)-plane for the completely convective shell ($\gamma_c = 1.0$) and different values of η and Γ_1 giving birth to several behaviors: limit-cycle (*diamonds*), pulsational stability (*dots*), and vibrational instability (*white regions*). (*a*) $\eta = 0.92$, $\Gamma_1 = 1.1$; (*b*) $\eta = 0.888$, $\Gamma_1 = 1.1$; (*c*) $\eta = 0.888$, $\Gamma_1 = 1.2$; and (*d*) $\eta = 0.888$, $\Gamma_1 = 1.3$. Eq. (1) has been used.

have investigated the role of the adiabatic exponent, Γ_1, as driving agent. From the mathematical perspective of the model, the question resides in establishing the relative effect on the system dynamics of the parameter γ_c, on one hand, and of the parameter Γ_1, on the other hand, included in the definition of the parameters $q \equiv m\Gamma_1 - 2$ and $d \equiv m(\Gamma_1 - 2)/2$. The case of a completely convective shell translates for this one-zone model into the disappearance of the κ-mechanism, with the driving being supplied only by the γ-mechanism. To test whether the pulsational instability of our convective models is due to the γ-mechanism or to a convection-induced driving mechanism, we studied the evolution of the limit-cycle region in the (ζ, ζ_c)-plane as Γ_1 is varied. The results obtained so far have used the value $\Gamma_1 = 1.1$, as employed by Stellingwerf (1986). We conjecture that if the obtained cases of self-sustained oscillations are a product of convection-induced driving, then the γ-mechanism has very little, if any, influence on their properties. Figures 10*a* and 10*b* display two cases of different shell thickness, concluding, as in § 3.1, that a thicker shell implies a wider range of parameters leading to pulsational instability. In the completely convective case, this increase causes a shift of the limit-cycle region to lower ζ_c. The same shift occurs by increasing the Γ_1 value at constant shell thickness or, in other words, by decreasing the efficiency of the γ-mechanism (Figs. 10*b*, 10*c*, and 10*d*). This means that convection and turbulent pressure are driving mechanisms for fully convective models, since the region where these models display a limit-cycle stability marginally depends on the adopted Γ_1 value. This finding supports the theoretical predictions by Xiong et al. (1998) concerning the driving provided by the coupling between pulsation and convection, but we also find that turbulent pressure is a destabilizing mechanism instead of a damping factor for pulsation. However, current models assume that the physical properties of the driving region can be described by a Kramers opacity law and by a very crude equation of state. Therefore, there is no guarantee that current models properly account for the thermodynamical and dynamical properties of the different partial ionization zones in low-density envelope regions.

5. CONCLUSIONS

In this paper we have thoroughly analyzed the one-zone convective model introduced by Stellingwerf (1986). The model appears in the form of a system of four ordinary differential equations in which the variables are the radius of the shell, the velocity, the pressure, and the convective velocity. The nonadiabaticity resides in the pressure, which is considered as a nonadiabatic perturbation of the reference pressure and thus can be considered as a nonadiabatic variable of the system. The model accounts for the self-excited oscillations by adopting a value for the adiabatic exponent Γ_1 that is close to unity. The main parameters of the system are the fraction γ_c of convective luminosity with respect to the total luminosity and the timescale ratios ζ and ζ_c, which are a measure of the dynamical timescale to the thermal timescale and to the convective timescale, respectively. We have extended the model by considering explicitly the role of the turbulent pressure and the case of a completely convective shell.

The one-zone models constructed by Stellingwerf (1986) were integrated only for a few dynamical timescales, and therefore the approach to limit-cycle stability remained still to be investigated. To properly identify the region of the parameter space that shows a limit-cycle behavior (pulsational instability), we have selected a parametric space given by $\gamma_c = 1$ and ζ, $\zeta_c \leq 10$. Our parametric study revealed well-defined regions where limit cycles exist, born through the Hopf bifurcation. For a typical shell thickness of 11%, pulsational instability was encountered only for the radiation-dominated cases ($\gamma_c < 0.5$), while the increase in the shell thickness displaces this limit to upper values of γ_c. The existence of these upper values supports the work by Stellingwerf (1986) and further strengthens the role played by convection as a damping mechanism.

Additionally, we have undertaken a parametric study to investigate the influence of the turbulent pressure on the overall dynamics of the system and implicitly on the existence of limit cycles. The turbulent pressure appears to be a driving mechanism, as the regions where the models approach a limit-cycle stability are more extended than for models that do not account for the turbulent pressure. Moreover and even more importantly, we find that one-zone models that account for turbulent pressure do not show a spurious peak along the rising branch of light curves. The inclusion of this term is also supported by the occurrence in the (ζ, ζ_c)-plane of a pulsationally unstable region bounded to the left and to the right by two pulsationally stable regions, as expected from physical considerations and hydrodynamic models. Moreover, the models located in this region display a morphology of the light curves and the velocity time series quite similar to those of nonlinear, hydrodynamic models and actual Cepheids.

As a natural continuation of the work by Stellingwerf (1986), we have investigated the vibrational and pulsational stability of completely convective models. Our predictions disclose a well-defined region of the parameter space where these red models approach a limit-cycle stability. The turbulent pressure appears to be a driving mechanism, a finding that supports the results originally brought forward by Ostlie & Cox (1986) and Cox & Ostlie (1993) on the basis of both linear and nonlinear LPV models but is at odds with predictions based on linear, convective models provided by Xiong et al. (1998). We computed several sequences of models by adopting different values of the adiabatic exponent and of the shell thickness. We found, in

agreement with Xiong et al. (1998), that the coupling between pulsation and convection is the key physical mechanism that drives the pulsation instability in these simple structures. We have also performed a qualitative comparison with empirical properties of LPVs. We have found some similarities, but only one feature partially agrees with empirical data: the maximum in the light curve is not correlated with the minimum in the velocity curve. However, the comparison with observations might be hampered by the occurrence of long secondary periods. We are not aware of detailed measurements of macroturbulent velocity along the pulsation cycle of LPVs; however, our models suggest that the maximum in the light curve takes place soon after the maximum in the convective velocity.

Current one-zone models account for the coupling between convection and pulsation and for turbulent pressure. We investigated the sensitivity to free parameters and to the physical assumptions adopted to construct the models. However, the treatment and the inclusion of these physical ingredients rely on crude physical approximations. A more detailed investigation is required before we can assess whether our current theoretical framework might mimic the complex pulsation behavior of LPVs, and this implies the use of the asymptotic perturbation theory to compute analytically the properties of the limit cycle. The pulsational behavior disclosed by these simple models for fully convective models will be addressed in a forthcoming paper on the basis of nonlinear, hydrodynamic models (A. Munteanu et al. 2005, in preparation).

It is a pleasure to thank P. Wood for a detailed reading of a draft of this manuscript and for several suggestions concerning the comparison between theory and observations. This work has been partially supported by MCYT grant AYA2002-04094-C03-01, by the European Union FEDER funds, and by the CIRIT. One of us, G. B., acknowledges partial support from INAF within the framework of the project "The Large Magellanic Cloud: A Laboratory for Stellar Astrophysics" and PRIN 2003 within the framework of the project "Continuity and Discontinuity in the Galaxy Formation." A. M. acknowledges a scholarship from UPC, which allowed her to conclude the present work.

APPENDIX

THE TURBULENT PRESSURE

In order to include the turbulent pressure and its associated energy terms in the present one-zone model, one must start from the equation of momentum and energy conservation for the treatment of convection of Stellingwerf (1982):

$$\frac{D\langle \boldsymbol{u} \rangle}{Dt} = -\frac{1}{\rho}\nabla(P + P_t) - \nabla\Phi, \tag{A1}$$

$$\frac{D}{Dt}(E + E_t) + (P + P_t)\frac{DV}{Dt} = -\frac{1}{\rho}\nabla(F_r + F_c + F_t). \tag{A2}$$

Here as well as throughout our work, we have used the notations employed in the original investigations. In Stellingwerf (1982), any quantity was written as $x = \langle x \rangle + x'$, where $\langle x \rangle$ was the mean quantity and x' the fluctuating part. In equation (A2), $D/Dt = (\partial/\partial t + \langle \boldsymbol{u} \rangle \cdot \nabla)$ is the Lagrangian time derivative, where u is the convective velocity, E is the specific internal energy, $V \equiv 1/\rho$ is the specific volume, P is the thermodynamic pressure, and

$$E_t \equiv \frac{1}{2}\left\langle (u')^2 \right\rangle, \tag{A3}$$

$$P_t \equiv \rho\left\langle (u')^2 \right\rangle, \tag{A4}$$

$$F_c \equiv \rho C_p \langle (u'T') \rangle, \tag{A5}$$

$$F_t \equiv \frac{1}{2}\left\langle (\boldsymbol{u}')^2 \boldsymbol{u} \right\rangle \tag{A6}$$

represent, respectively, the convective energy, the turbulent pressure, and the convective and turbulent kinetic fluxes, as defined in Stellingwerf (1982). These equations must be adapted to the one-zone model. The momentum equation translates into

$$\frac{d^2X}{d\tau^2} = (1 - \alpha_p)X^{-q}h + \alpha_p X^{-c}U_c^2 - X^{-2}, \tag{A7}$$

where equation (5) has been used and the parameters are $q \equiv m\Gamma_1 - 2$, $c \equiv m - 2$, and

$$\alpha_p \equiv \frac{P_{t_0}}{P_0 + P_{t_0}} = \frac{X_0^{-m}U_{c_0}^2}{X_0^{-m\Gamma_1}h_0 + X_0^{-m}U_{c_0}^2}. \tag{A8}$$

To ease the calculation, the energy equation can be divided into

$$\frac{\partial(L_r + L_c)}{\partial m} = \frac{\Gamma_1 P}{\rho^2(\Gamma_3 - 1)} \frac{\partial \rho}{\partial t} \frac{1}{\rho(\Gamma_3 - 1)} \frac{\partial P}{\partial t}, \tag{A9}$$

$$\frac{\partial L_t}{\partial m} = \frac{P_t}{\rho^2} \frac{\partial \rho}{\partial t} - \frac{\partial E_t}{\partial t}. \tag{A10}$$

In the determination of the convective and turbulent luminosities, one can use the conservative choice of L_c of equation (27) of Stellingwerf (1986) and equation (A6) of the present work. The calculations lead to an expression for L_t identical to that of L_c, that is, $L_t = X^{-c} U_c^3$, while $E_t = U_c^2/2$. Using equations (A9) and (A10), one can get the final equation of energy conservation taking into account the turbulence:

$$\frac{dh}{d\tau} = -m \frac{\alpha_p(\Gamma_3 - 1)}{1 - \alpha_p} X^{2d-1} \frac{dX}{d\tau} U_c^2 - \frac{\rho_0(\Gamma_3 - 1)}{P_0} \zeta_c \left(X^d h^{1/2} U_c - X^{2d} U_c^2 \right) - \zeta X^{2d} \left[\gamma_r X^b h^{s+4} + (1 - \gamma_r) X^{-c} U_c^3 - 1 \right], \tag{A11}$$

where $d \equiv m(\Gamma_1 - 1)/2$ and $\gamma_r \equiv L_{r_0}/L_0$. All the other symbols used in equation (A11) have their usual meaning. The equation for the convective velocity coincides with the zero turbulence case, as the approximation made for its recovery uses the temperature as a function of the thermodynamic pressure only. In the case in which the turbulent energy, E_t, is neglected in equation (A2), equation (A11) becomes

$$\frac{dh}{d\tau} = -m \frac{\alpha_p(\Gamma_3 - 1)}{1 - \alpha_p} X^{2d-1} \frac{dX}{d\tau} U_c^2 - \zeta X^{2d} \left[\gamma_r X^b h^{s+4} + (1 - \gamma_r) X^{-c} U_c^3 - 1 \right]. \tag{A12}$$

Thus, to a first approximation, the one-zone convective model with turbulent pressure is described by equations (A7) and (A12), while for the convective velocity equation (1) remains valid.

REFERENCES

Baker, N. 1966, in Stellar Evolution, ed. R. F. Stein & A. G. W. Cameron (New York: Plenum), 333
Bono, G., Castellani, V., & Marconi, M. 2000, ApJ, 529, 293
———. 2002, ApJ, 565, L83
Bono, G., Gieren, W. P., Marconi, M., Fouqué, P., & Caputo, F. 2001, ApJ, 563, 319
Bono, G., Marconi, M., & Stellingwerf, R. F. 1999, ApJS, 122, 167
Bono, G., & Stellingwerf, R. F. 1994, ApJS, 93, 233
Buchler, J. R. 1998, in ASP Conf. Ser. 135, A Half Century of Stellar Pulsation Interpretation: A Tribute to Arthur N. Cox, ed. P. A. Bradley & J. A. Guzik (San Francisco: ASP), 220
Buchler, J. R., & Kovacs, G. 1986, ApJ, 308, 661
Christensen-Dalsgaard, J., Kjeldsen, H., & Mattei, J. A. 2001, ApJ, 562, L141
Cox, A. N., & Ostlie, D. A. 1993, Ap&SS, 210, 311
Cox, J. P. 1980, Theory of Stellar Pulsation (Princeton: Princeton Univ. Press)
Dolphin, A. E., et al. 2002, AJ, 123, 3154
Dziembowski, W., & Kovacs, G. 1984, MNRAS, 206, 497
Dziembowski, W. A., Gough, D. O., Houdek, G., & Sienkiewicz, R. 2001, MNRAS, 328, 601
Edmonds, P. D., & Gilliland, R. L. 1996, ApJ, 464, L157
Feuchtinger, M., Buchler, J. R., & Kolláth, Z. 2000, ApJ, 544, 1056
Fox, M. W., & Wood, P. R. 1982, ApJ, 259, 198
Gough, D. O. 1967, AJ, 72, 799
Hinkle, K. H., Hall, D. N. B., & Ridgway, S. T. 1982, ApJ, 252, 697
Hinkle, K. H., Lebzelter, T., Joyce, R. R., & Fekel, F. C. 2002, AJ, 123, 1002
Hinkle, K. H., Scharlach, W. W. G., & Hall, D. N. B. 1984, ApJS, 56, 1
Icke, V., Frank, A., & Heske, A. 1992, A&A, 258, 341
Ishida, T., & Takeuti, M. 1991, Ap&SS, 178, 311
Ita, Y., et al. 2004, MNRAS, 347, 720
Keller, S. C., & Wood, P. R. 2002, ApJ, 578, 144
Kervella, P., Coudé du Foresto, V., Perrin, G., Schöller, M., Traub, W. A., & Lacasse, M. G. 2001, A&A, 367, 876
Kiss, L. L., & Bedding, T. R. 2003, MNRAS, 343, L79
Lebzelter, T., & Hinkle, K. H. 2002, A&A, 393, 563
Lebzelter, T., Kiss, L. L., & Hinkle, K. H. 2000, A&A, 361, 167
Monelli, M., et al. 2003, AJ, 126, 218
Ostlie, D. A., & Cox, A. N. 1986, ApJ, 311, 864
Petroni, S., Bono, G., Marconi, M., & Stellingwerf, R. F. 2003, ApJ, 599, 522
Saitou, M. 1993, Ap&SS, 210, 355
Saitou, M., Takeuti, M., & Tanaka, Y. 1989, PASJ, 41, 297
Stellingwerf, R. F. 1972, A&A, 21, 91
———. 1982, ApJ, 262, 330
———. 1986, ApJ, 303, 119
Stellingwerf, R. F., & Donohoe, M. 1986, ApJ, 306, 183
Stellingwerf, R. F., Gautschy, A., & Dickens, R. J. 1987, ApJ, 313, L75
Tanaka, Y. 2001, in Stellar Pulsation–Nonlinear Studies, ed. M. Takeuti & D. D. Sasselov (Dordrecht: Kluwer), 155
Unno, W., & Xiong, D. R. 1990, in Progress of Seismology of the Sun and Stars, ed. Y. Osaki & H. Shibahashi (Berlin: Springer), 103
———. 1993, Ap&SS, 210, 77
Usher, P. D., & Whitney, C. A. 1968, ApJ, 154, 203
Wood, P. R. 2000, in IAU Colloq. 176, The Impact of Large-Scale Surveys on Pulsating Star Research, ed. L. Szabados & D. Kurtz (ASP Conf. Ser. 203; San Francisco: ASP), 379
Wood, P. R., Olivier, E. A., & Kawaler, S. D. 2004, ApJ, 604, 800
Xiong, D. R., Deng, L., & Cheng, Q. L. 1998, ApJ, 499, 355
Yecko, P. A., Kollath, Z., & Buchler, J. R. 1998, A&A, 336, 553